Journal of Applied Physics

Charge trapping at Fe due to midgap levels in Ga_2O_3

Cite as: J. Appl. Phys. **129**, 085703 (2021); https://doi.org/10.1063/5.0042622
Submitted: 01 January 2021 . Accepted: 10 February 2021 . Published Online: 24 February 2021

Suman Bhandari, and M. E. Zvanut

Journal of Applied Physics | ARTICLE | scitation.org/journal/jap

Charge trapping at Fe due to midgap levels in Ga_2O_3

Cite as: J. Appl. Phys. **129**, 085703 (2021); doi: 10.1063/5.0042622
Submitted: 1 January 2021 · Accepted: 10 February 2021 ·
Published Online: 24 February 2021

View Online Export Citation CrossMark

Suman Bhandari[a] and M. E. Zvanut

AFFILIATIONS

Department of Physics, University of Alabama at Birmingham, 1300 University Blvd., Birmingham, Alabama 35233, USA

[a]**Author to whom correspondence should be addressed:** omus1987@uab.edu

ABSTRACT

Fe acts as an electron trap in gallium oxide (Ga_2O_3), thereby producing a semi-insulating material that can be used in device fabrication. However, such trapping can lead to negative effects when Fe is unintentionally incorporated into bulk crystals or thin films. In this work, photoinduced electron paramagnetic resonance (photo-EPR) is used to investigate carrier capture at Fe in β-Ga_2O_3. Two crystals doped with 8×10^{17} cm^{-3} and 5×10^{18} cm^{-3} Fe and one Mg-doped crystal containing 7×10^{16} cm^{-3} unintentional Fe are studied by illuminating with LEDs of photon energies 0.7–4.7 eV. Steady state photo-EPR results show that electrons excited from Ir, an unintentional impurity in bulk crystals, are trapped at Fe during illumination with photon energy greater than 2 eV. Significantly, however, trapping at Fe also occurs in the crystals where Ir does not participate. In such cases, we suggest that excitation of intrinsic defects such as oxygen or gallium vacancies are responsible for trapping of carriers at Fe. The results imply that the investigation of intrinsic defects and their interaction with Fe is necessary to realize stable and reliable Ga_2O_3:Fe devices.

INTRODUCTION

Gallium oxide (Ga_2O_3) is an ultra-wide bandgap (4.6–4.9 eV) semiconductor with an estimated breakdown field of 8 MV/cm and intrinsic carrier mobility limit of 300 $cm^2/(V\,s)$.[1,2] These properties, along with the availability of large-scale potentially low-cost native substrates, make Ga_2O_3 a more promising candidate for power electronics than conventional wide-bandgap semiconductors such as GaN and SiC. Several bulk growth melt methods such as float zone, Czochralski, and edge-defined film-fed growth are viable, but most employ Ir crucibles. As a consequence, Ir, along with several other elements, becomes unintentionally incorporated during growth, leading to potentially deleterious effects on the electrical properties. For example, Si contributes to the as-grown n-type conductivity of the material and Ir, which forms a defect level in the middle of the bandgap, could act as an efficient recombination center.[3,4]

Another important impurity in Ga_2O_3 is Fe, which is used to control the as-grown n-type conductivity. The Fe dopant presumably acts as a compensating acceptor, capturing the free electrons generated during growth, thereby reducing the conductivity of the intrinsic material.[5] Today, most semi-insulating Ga_2O_3 is achieved by doping with Fe, and prototype high power devices are being developed.[2] However, Fe is also an unintentional impurity in both undoped bulk crystals and homoepitaxially grown films.[3,6–10] For instance, there are several reports of Fe incorporation into the epitaxial layer grown on Fe-doped Ga_2O_3 substrates during growth.[7–10] Incorporation of the acceptor into epitaxial films can lead to unintentional compensation, thereby negatively affecting the device.[8–10] The work by McGlone *et al.*, for example, demonstrates that the Fe_{Ga} trap level causes threshold voltage instabilities in Ga_2O_3 transistors grown on Fe-doped Ga_2O_3 substrates.[8]

Despite the significance of Fe-related trapping in Ga_2O_3, there is little spectroscopic evidence for carrier capture at the Fe impurity, and most of the work considers only the effect of ionized impurities in bulk crystals. For example, electron paramagnetic resonance (EPR) measurements demonstrate the trapping at Fe in Ga_2O_3 by showing a simultaneous change in the amount of Fe^{3+} and Ir^{4+} during illumination.[11,12] In device-grade epitaxial films where unintentional impurities should be minimal, intrinsic point defects are likely to be the most significant contribution to carrier capture at Fe. Since oxygen vacancies (V_O), gallium vacancies (V_{Ga}), and their complexes are predicted to be thermodynamically stable, particularly under n-type conditions that are typical for Ga_2O_3 growth, their presence could lead to excess carrier generation under external excitation and subsequent trapping by dopants.[13–16] Yet, evidence for interaction between the seemingly omnipresent Fe and intrinsic defects is lacking.

In this work, we report the effects of defects on the stability of the Fe^{3+} charge state, an important dopant used to produce semi-insulating Ga_2O_3 material for power devices. We probe a specific charge state of a variety of defects using EPR and, with a modified version of optical absorption that employs EPR, we monitor the defect and its charge transitions. To obtain a complete picture of the possible charge transfer paths for Fe, we study two Fe-doped samples that vary in Fe concentration by almost an order of magnitude and have a Fermi level (E_F) in the upper half of the bandgap. The study also includes a Mg-doped crystal, another possible path for production of semi-insulating substrates. The Mg-doped sample contains 7×10^{16} cm^{-3} unintentionally incorporated Fe and a Fermi level in the lower half of the bandgap. Besides Ir, which is a major concern in bulk growth, the study shows that intrinsic defects inherent to both bulk and thin film Ga_2O_3 must be contributing to the observed carrier trapping at the Fe impurity.

EXPERIMENTAL DETAILS

Photo-EPR experiments were performed on two Fe-doped (FeGox and HFeGox) and one Mg-doped (MgGox) β-Ga_2O_3 crystals grown by the Czochralski method. The samples HFeGox and MgGox were cut from boules of Fe-doped Ga_2O_3 and Mg-doped Ga_2O_3, which were analyzed by glow discharge mass spectroscopy (GDMS) to estimate the amount of different impurities. The concentrations of Fe, Mg, Si, and Cr in FeGox and MgGox were determined by secondary ion mass spectrometry (SIMS). Table I summarizes the results obtained from each measurement. Since the Ir concentration determined by SIMS is uncalibrated due to the lack of a standard and GDMS was not performed on the FeGox sample, we have no reliable measure of the total Ir concentration in this sample. However, we estimate that at least 3×10^{17} cm^{-3} Ir is present from the amount of Ir^{4+} detected using EPR as explained below.

An EPR signal was integrated twice numerically to obtain the integrated intensity and was then compared with that of a calibrated Si:P powder to obtain the total amount of the EPR-active center.[17] The calculated amount is accurate to no more than 50%. The average concentration throughout the sample was obtained by dividing by the volume of the sample. For FeGox, the minimum concentration of Ir was estimated as 3×10^{17} cm^{-3} by calculating the number of Ir^{4+} spins generated after the sample was illuminated with a 2.64 eV LED with a flux of 3×10^{16} photons/s for 25 min. For MgGox, the EPR-estimated Ir^{4+} concentration (7×10^{17} cm^{-3}) agrees reasonably with the GDMS value, given the factor of 2 uncertainty of the EPR-estimated numbers. No Ir^{4+} was observed in HFeGox. Due to the complexity of the Fe^{3+} EPR signal, the total number of centers could not be determined using the Si:P standard. Rather, the Fe^{3+} intensity in the Mg-doped (MgGox) sample was approximated as the SIMS concentration of Fe for that sample. Here, we assume that all the Fe is substitutional and is in the 3+ state. The Fe^{3+} intensity in MgGox was then used for comparison with the Fe^{3+} intensity in other samples.

The samples were 450 μm thick, 1.0 cm long, and 0.2 cm wide. X-ray diffraction was performed to determine the orientation. The *b* axis is the surface normal to the largest face (010), while the *c* axis is nearly parallel to the length of the sample. Since an EPR signal represents a defect in a specific charge state, any change in the EPR amplitude represents a change in the charge state of the defect. In order to investigate charge transitions of impurities, we performed photo-EPR experiments at 9.4 GHz using light emitting diodes (LEDs) of photon energy from 0.7 to 4.7 eV. All measurements were carried out at 30 K with the magnetic field perpendicular to the *b* axis in a plane nearly perpendicular to the *c* axis. For steady state photo-EPR, a dark spectrum was obtained before the sample was illuminated. Then, the sample was illuminated until the EPR signal nearly saturated, and a spectrum was taken before turning off the LED. We call this spectrum "after illumination." We then changed wavelengths and continued the process up to 2.3 eV. For photon energy ≥2.3 eV, where the signal began to change substantially, the signal was returned to approximately the initial dark amplitude by illuminating at 1.9 eV with a flux of 1×10^{17} photons/s for 20 min. A new "dark" spectrum was obtained before proceeding to the next wavelength. This 1.9 eV restoring step followed by illumination at a selected wavelength continued through the remainder of the bandgap. After acquiring the steady state EPR signal for each photon energy, the relative change in the number of centers was calculated by comparing the EPR amplitudes before and after illumination. The total number of defects was calculated as explained earlier using the signal with the largest amplitude. Then, by comparing the EPR amplitudes with the remaining spectra, the number of centers for all other photon energies was calculated. A nearly constant photon flux (3×10^{16} photons/s) was maintained until 3.5 eV for each photon energy by using neutral density filters. Above 3.5 eV, ~1×10^{15} photons/s was used due to limited power of the LEDs.

TABLE I. Impurity concentrations, 10^{17} cm^{-3}, in Ga_2O_3 crystals measured by SIMS (FeGox and MgGox) and GDMS (HFeGox and MgGox).

	FeGox, SIMS	HFeGox, GDMS	MgGox, GDMS (SIMS)
[Fe]	8.0	50	7.0 (0.7)
[Mg]	0.02	5.0	20 (25)
[Ir]	…	2.0	3.0 (…)
[Si]	1.0	20	10 (2.8)
[Cr]	0.18	0.55	0.7 (0.1)

RESULTS

The EPR signature of Fe^{3+} in Ga_2O_3 is well-known.[18,19] Figure 1(a) shows the Fe^{3+} spectrum acquired from a Fe-doped sample (FeGox) at 30 K with the magnetic field perpendicular to the *b* axis in a plane nearly perpendicular to the *c* axis. The inset shows the EPR spectrum of Ir^{4+}, recently identified in Ga_2O_3, obtained after the sample was irradiated with 2.64 eV.[11] Consistent with earlier observations, Ir^{4+} is not present in the dark; however, it is observed after the sample is illuminated with photon energy greater than 2 eV. The Fe^{3+} and Ir^{4+} spectra before (dashed) and after (solid) the 2.64 eV

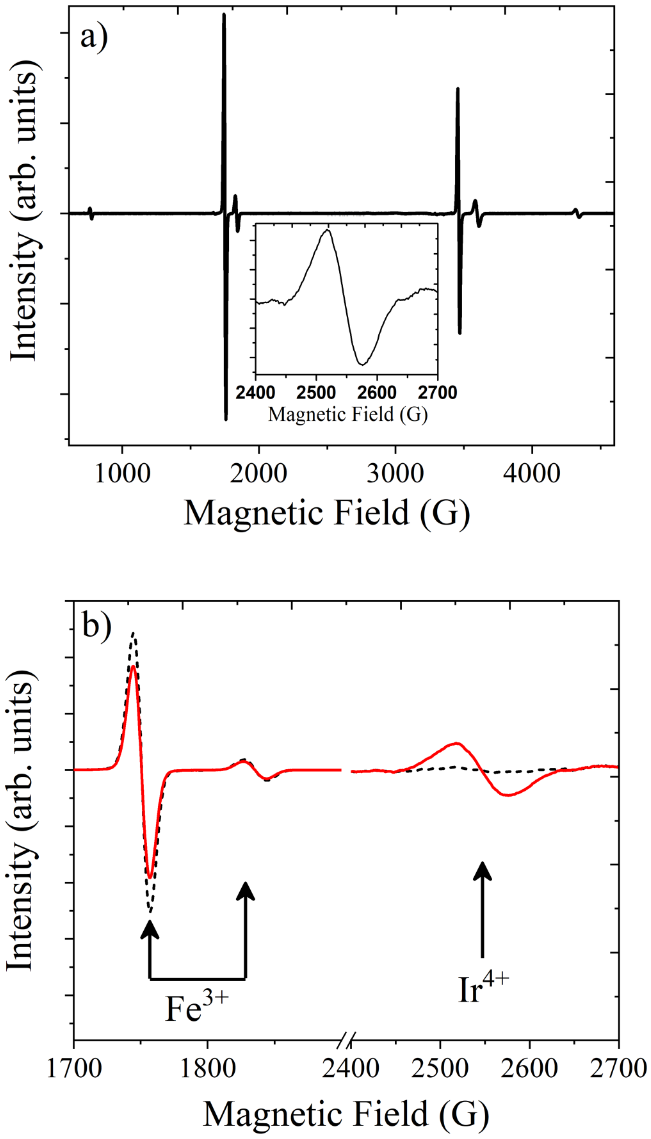

FIG. 1. (a) EPR spectra of Fe^{3+} in FeGox; inset: EPR spectrum of Ir^{4+}in the FeGox sample after 2.64 eV irradiation. (b) EPR spectra of $Fe^{3+}$and Ir^{4+}, as indicated, before (dashed) and after (solid) illumination with the 2.64 eV. The spectra were acquired at 30 K with magnetic field perpendicular to the *b* axis in a plane nearly perpendicular to *c* axis.

illumination are shown in Fig. 1(b). All Fe^{3+} lines respond to the light similarly, so only the low field Fe^{3+} lines near 1800 G are illustrated here for clarity. To obtain the optimum signal, Ir^{4+} spectra were taken with larger modulation amplitude (10 G) and microwave power (10 mW) as compared to Fe^{3+} (5 G and 0.1 mW). The change in the EPR amplitudes implies a change in the charge state of a defect so that the decrease of Fe^{3+} and increase of Ir^{4+} with irradiation suggests charge transfer between Fe^{3+} and Ir^{4+}.

The 30 K steady state photo-EPR data demonstrating the effect of each photon energy on Fe^{3+} (unfilled triangles) and Ir^{4+} (filled circles) in the FeGox sample are shown in Fig. 2. The vertical axis represents the change in the concentration of Fe^{3+} or Ir^{4+} after each photon energy. Above 2 eV, Ir^{4+} increases when Fe^{3+} decreases, clearly suggesting that one is affected by the other. The changes become less pronounced above 3.5 eV, due to the limited photon flux available in the higher photon energy sources. Consistent with the predicted $Ir^{3+/4+}$ level of ∼2.3 eV below the conduction band minimum (CBM),[4] the 2.3 eV photo-threshold suggests that electrons are excited from Ir^{3+} to the conduction band, resulting in an increase in the amount of Ir^{4+}. The electron is subsequently captured by Fe^{3+}, decreasing the amount of Fe^{3+}. Although the relative uncertainty between points is less than the size of the symbols, the uncertainty in the absolute change is at least a factor of two as indicated by the error bar. Therefore, the apparent one-to-one relationship suggested by the figure may be fortuitous. Possibly other defects, predicted to have defect levels that lie in the midgap, also contribute to electron excitation and trapping by Fe.

The contribution of defects other than Ir is tested by performing experiments on different types of samples: a heavily Fe-doped (HFeGox) sample that contains six times more Fe than FeGox and a Mg-doped (MgGox) sample that contains unintentional Fe (7×10^{16} cm^{-3}). The photo-EPR Fe^{3+} response in the former is expected to be similar to the other Fe-doped sample, and the Fe^{3+} in the latter should decrease only slightly or not at all since most of the Ir should be in the 4+ charge state. In Fig. 3, we show the steady state photo-EPR of Fe^{3+} in HFeGox (unfilled triangles), and Fe^{3+} (filled triangles) and Ir^{4+} (filled circles) in MgGox samples. As

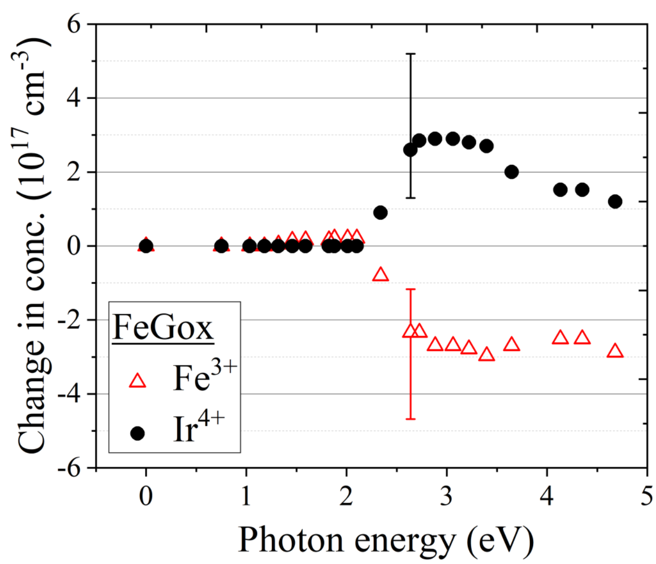

FIG. 2. Steady state photo-EPR of Fe^{3+}(unfilled triangles) and Ir^{4+}(filled circles) in FeGox at 30 K. The error bars show the absolute error in the concentration. The relative error is less than the size of the symbols. A flux of 3×10^{16} photons/s was used below 3.5 eV. The flux above 3.5 eV was limited to 1×10^{15} photons/s due to limited power of the LEDs.

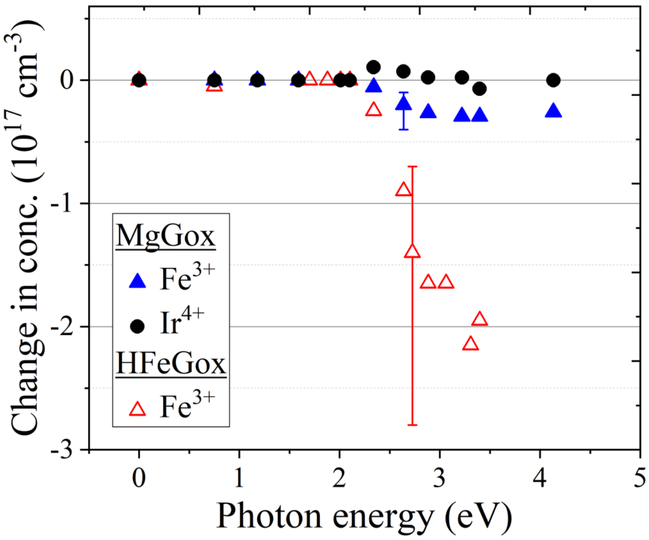

FIG. 3. Steady state photo-EPR of Fe^{3+} (filled triangles) and Ir^{4+} (filled circles) in MgGox and Fe^{3+} in HFeGox (unfilled triangles) at 30 K. The error bars show the absolute error in the concentration. The relative error is less than the size of the symbols.

observed in the FeGox sample, Fe^{3+} (triangles) decreases above 2 eV in these samples. Surprisingly, however, Ir^{4+} is never observed in HFeGox indicating that a photo-excited Ir-electron cannot be the source of the Fe^{3+} decrease in this sample. Although why Ir is not seen is not clear, the results unequivocally indicate that other species must contribute to charge trapping at the Fe impurity. The results for the Mg-doped sample are equally surprising. Although the change in Fe^{3+} is less than that seen in the Fe-doped samples, it is larger than any changes in Ir. At several photon energies, there were no changes in the Ir^{4+} EPR signal. The photo-EPR results from the heavily Fe-doped sample and Mg-doped sample confirm that Ir alone is not responsible for the decrease of Fe^{3+}, and thus, other defects must contribute electrons to Fe^{3+}.

We note that in contrast to that observed in FeGox, below 2 eV, the Fe^{3+} (triangles) concentration remains unchanged in the HFeGox and MgGox samples. The results from HFeGox and MgGox are consistent with our earlier interpretation of this energy region as photo-excitation from the $Fe^{2+/3+}$ defect level.[12] The absence of an increase in Fe^{3+} in the heavily Fe-doped sample is expected because photo-excitation is competing with the recapture of the photo-excited carrier. In this 5×10^{18} cm^{-3} Fe-doped sample, there are so many Fe^{3+} sites that the recombination process is much faster than the EPR detection time and no change can be observed. In the Mg-doped sample, the Fe^{2+} to Fe^{3+} transition is not observed due to the almost null presence of Fe^{2+}, as E_F is thought to be significantly below the $Fe^{2+/3+}$ level.[12,20–22]

DISCUSSION

Before any illumination, the dominant signal in all of the samples is Fe^{3+}. As discussed above, the photo-EPR data for the FeGox sample show that electrons are excited from Ir^{3+} to CBM and subsequently captured by Fe^{3+}during illumination with energy greater than 2 eV. In our previous work, we used photo-EPR data to support the interpretation of the photo-threshold as the $Ir^{3+/4+}$ level, 2.3 eV below CBM.[23] We do not discuss the determination of the $Ir^{3+/4+}$ level further. Rather, the primary concern is the possible presence of defects other than Ir that affect Fe^{3+} transitions.

In HFeGox, with six times more Fe than FeGox discussed above, the Fe^{3+} decreases at photon energies greater than 2 eV (unfilled triangles in Fig. 3) with no contribution from Ir. In fact, Ir^{4+} is not observed either before or after irradiation with any photon energy. This is a strong indication that besides Ir, defects that have levels similar to Ir are photo-ionized to contribute electrons to Fe. In the Mg-doped sample, Fe^{3+} decreases, again with no or minimal change in the Ir^{4+} concentration. Here, the E_F lies below the $Ir^{3+/4+}$ level so that a null change in Ir^{4+} via excitation of an electron to the conduction band is expected due to the absence of Ir^{3+}. However, the question remains as to what other charge transfer mechanisms are responsible for the ionization of Fe.

We scanned the magnetic field range in each sample to search for additional centers that may contribute to the changes observed in the Fe^{3+}. While there are few lines not associated with Fe^{3+} and Ir^{4+}, their total intensity is not sufficient to contribute to the changes seen in Fe^{3+}, with one exception. In the heavily doped sample (HFeGox), there is one 200 G wide EPR absorption near $g \sim 2.28$, which could be related to the decrease in the amount of Fe^{3+} observed in that sample. The concentration of the defect represented by this signal is on the order of 10^{18} cm^{-3}. The resonance is not the same as any of the recently reported intrinsic defects such as V_{Ga} or IR1 or EPR1, nor is it present in any of the other samples, including the more lightly Fe-doped sample (FeGox).[24–26] We speculate that the center is an Fe complex induced by the high Fe concentration. Although the large linewidth makes photoinduced changes difficult to quantify, we do see an increase in this signal over the same photon energy range where the Fe^{3+} decrease is observed, reinforcing the possibility of charge transfer to the isolated substitutional Fe.

In the Mg-doped sample, there are no other EPR lines that could directly account for the Fe^{3+} decrease; however, we can suggest possible charge transitions based on the position of the E_F in this sample and the various published values of defect levels. Experimental work suggests that the $Mg^{-/0}$ level is 0.65 eV above the valence band maximum (VBM) while density functional theory (DFT) calculations place the level 1.3 eV above VBM.[21,22] As mentioned earlier $Ir^{3+/4+}$ is thought to be ∼2.6 eV above VBM.[4] Since we do not observe the EPR-active Mg^0 and do detect Ir^{4+}, we place E_F somewhere between 0.6 and 2.6 eV above VBM. Defect levels for the various vacancies span a wide range from 1.9 to 4.1 eV above VBM.[13,14] Thus, an electron could be photo-excited from one of the filled vacancy levels to the conduction band or from the valence band edge to an empty vacancy level. In the former, the vacancy would play a similar role as Ir in the FeGox sample. In the latter case, the hole created by excitation from valance band to the vacancy could be captured at the $Fe^{3+/4+}$ level. However, since we never see the Mg^0 EPR signal, the $Mg^{-/0}$ level would have to lie below the $Fe^{3+/4+}$ in order for hole capture to occur preferentially at Fe. Interestingly, the experimental work by Lenyk *et al.*[22] and Gustafson *et al.*[27] do place the $Mg^{-/0}$ level slightly (0.05 eV) below $Fe^{3+/4+}$, but with such a minimal difference, neutral Mg would likely compete with Fe for hole capture and the EPR signal should be detected. Furthermore, the level ordering contradicts the DFT calculated $Mg^{-/0}$ transition of 1.3 eV above VBM, which is ∼0.7 eV above the DFT predicted $Fe^{3+/4+}$ level.[21] Thus, excitation of an electron from a midgap defect seems the more likely transition.

While the specific types of defects responsible for charge exchange with Fe^{3+} are not clear from this study, the work does conclusively demonstrate that the centers must have levels near the middle of the Ga_2O_3 bandgap. As mentioned, several theoretical and experimental reports show that there are multiple trapping centers near midgap and most are attributed to intrinsic defects, like the single vacancy centers V_O or V_{Ga}.[13,14] Either the neutral V_O or neutral $V_{Ga(I)}$ and/or singly ionized $V_{Ga(II)}$ could be ionized by the >2 eV light and the free electron subsequently captured by Fe^{3+}.[13,14] Despite having been grown under oxygen rich conditions, which have been predicted to favor formation of V_{Ga}, we believe that V_O are the more likely source of the trapped electrons in our samples. Gallium vacancies, although detected in Ga_2O_3 by EPR and positron annihilation spectroscopy,[24–26,28] are not observed during our experiments due to the relatively low excitation energy used. The work of others shows that transformation from an EPR-silent to EPR-active charge state of a V_{Ga} requires extreme conditions.[24–26] For instance, Skachkov *et al.* used highly energetic electron (20 MeV) or proton (12 MeV) irradiation to a fluence of 10^{16} cm^{-2} to observe singly or doubly ionized V_{Ga}.[26] Although the fluence in our experiments is as high as 10^{19} cm^{-2}, the bandgap photon energy does not compare to the MeV energy used by others. Since we were unable to change the charge state of a V_{Ga}, the defect could hardly be the source of the electrons trapped at the Fe^{3+}. If one makes the reasonable assumption that charge injection in devices is more comparable to photo-excitation than particle irradiation, then one might not expect V_{Ga} to be responsible for trapping at Fe in Ga_2O_3 device structures either. Rather, oxygen vacancies or related defects are a more likely source. Indeed, V_O would make a very efficient charge transfer agent due to the negative U behavior.[13] Only the 2+ or neutral charge states are predicted to be stable; thus, two Fe^{3+} impurities could be compensated by only one V_O. Furthermore, since +1 is the EPR-active charge state for V_O, there would be no EPR signal, consistent with our results. Finally, note that consideration of V_O over V_{Ga} does not contradict the O-rich growth conditions since we are not claiming that there are more V_O than V_{Ga}, only that we can more easily ionize V_O compared to V_{Ga}.

In summary, we observe a decrease in the amount of Fe^{3+} in Ga_2O_3 crystals during illumination with photon energy greater than 2 eV and show that Fe^{3+} acts as a trapping center in the presence of energetic electrons. Importantly, the carrier capture can occur without change in the concentration of other identifiable impurities. Rather, we suggest that Fe-induced complexes in the case of heavily Fe-doped sample or isolated intrinsic defects in the case of Mg-doped sample are responsible for trapping at the substitutional Fe impurity. Evaluating contributions from intrinsic defects to electron capture at Fe is particularly important for the production of stable and reliable Ga_2O_3:Fe devices.

ACKNOWLEDGMENTS

The National Science Foundation (NSF) (Grant No. DMR-1904325) supported the work. John Blevins at Air Force Research Laboratory provided the lightly Fe-doped Ga_2O_3 sample and Jacob Leach, Kyma Inc., and Luke Sande, NG Synoptics, provided the heavily Fe-doped and Mg-doped Ga_2O_3 samples.

DATA AVAILABILITY

The data that support the findings of this study are available within the article.

REFERENCES

[1] M. Higashiwaki, K. Sasaki, A. Kuramata, T. Masui, and S. Yamakoshi, "Gallium oxide (Ga_2O_3) metal-semiconductor field-effect transistors on single-crystal β-Ga_2O_3 (010) substrates," Appl. Phys. Lett. **100**, 013504 (2012).

[2] S. J. Pearton, J. Yang, P. H. Cary, F. Ren, J. Kim, M. J. Tadjer, and M. A. Mastro, "A review of Ga_2O_3 materials, processing, and devices," Appl. Phys. Rev. **5**, 011301 (2018).

[3] A. Kuramata, K. Koshi, S. Watanabe, Y. Yamaoka, T. Masui, and S. Yamakoshi, "High-quality β-Ga_2O_3 single crystals grown by edge-defined film-fed growth," Jpn. J. Appl. Phys. **55**, 1202A2 (2016).

[4] J. R. Ritter, J. Huso, P. T. Dickens, J. B. Varley, K. G. Lynn, and M. D. McCluskey, "Compensation and hydrogen passivation of magnesium acceptors in β-Ga_2O_3," Appl. Phys. Lett. **113**, 052101 (2018).

[5] A. Kuramata, K. Koshi, S. Watanabe, Y. Yamaoka, T. Masui, and S. Yamakoshi, "Bulk crystal growth of Ga_2O_3," in *Proceedings of Oxide-Based Materials and Devices IX (SPIE OPTO)*, San Francisco, CA (SPIE, 2018), Vol. 10533.

[6] Z. Galazka, R. Uecker, K. Irmscher, M. Albrecht, D. Klimm, M. Pietsch, M. Brutzam, R. Bertram, S. Ganschow, and R. Fornari, "Czochralski growth and characterization of β-Ga_2O_3 single crystals," Cryst. Res. Technol. **45**, 1229 (2010).

[7] M. H. Wong, K. Sasaki, A. Kuramata, S. Yamakoshi, and M. Higashiwaki, "Anomalous Fe diffusion in Si-ion-implanted β–Ga_2O_3 and its suppression in Ga_2O_3 transistor structures through highly resistive buffer layers," Appl. Phys. Lett. **106**, 032105 (2015).

[8] J. F. McGlone, Z. Xia, C. Joishi, S. Lodha, S. Rajan, S. Ringel, and A. R. Arehart, "Identification of critical buffer traps in Si δ-doped β-Ga_2O_3 MESFETs," Appl. Phys. Lett. **115**, 153501 (2019).

[9] A. Mauze, Y. Zhang, T. Mates, F. Wu, and J. S. Speck, "Investigation of unintentional Fe incorporation in (010) β-Ga_2O_3 films grown by plasma-assisted molecular beam epitaxy," Appl. Phys. Lett. **115**, 052102 (2019).

[10] C. Joishi, Z. Xia, J. McGlone, Y. Zhang, A. R. Arehart, S. Ringel, S. Lodha, and S. Rajan, "Effect of buffer iron doping on delta-doped β-Ga_2O_3 metal semiconductor field effect transistors," Appl. Phys. Lett. **113**, 123501 (2018).

[11] C. A. Lenyk, N. C. Giles, E. M. Scherrer, B. E. Kananen, L. E. Halliburton, K. T. Stevens, G. K. Foundos, J. D. Blevins, D. L. Dorsey, and S. Mou, "Ir^{4+} ions in β-Ga_2O_3 crystals: An unintentional deep donor," J. Appl. Phys. **125**, 045703 (2019).

[12] S. Bhandari, M. E. Zvanut, and J. B. Varley, "Optical absorption of Fe in doped Ga_2O_3," J. Appl. Phys. **126**, 165703 (2019).

[13] J. B. Varley, J. R. Weber, A. Janotti, and C. G. Van de Walle, "Oxygen vacancies and donor impurities in β-Ga_2O_3," Appl. Phys. Lett. **97**, 142106 (2010).

[14] P. Deak, Q. D. Ho, F. Seemann, B. Aradi, M. Lorke, and T. Frauenheim, "Choosing the correct hybrid for defect calculations: A case study on intrinsic carrier trapping in β-Ga_2O_3," Phys. Rev. B **95**, 075208 (2017).

[15] J. B. Varley, H. Peelaers, A. Janotti, and C. G. Van deWalle, "Hydrogenated cation vacancies in semiconducting oxides," J. Phys.: Condens. Matter **23**(9), 334212 (2011).

[16]P. Weiser, M. Stavola, W. B. Fowler, Y. Qin, and S. Pearton, "Structure and vibrational properties of the dominant O-H center in β-Ga_2O_3," Appl. Phys. Lett. **112**, 232104 (2018).
[17]J. Weil and J. Bolton, *Electron Paramagnetic Resonance Elementary Theory and Practical Applications* (John Wiley & Sons, Inc., 2007), pp. 545–546.
[18]M. L. Meil'man, "EPR of Fe^{3+} ions in β-Ga_2O_3 crystals," Sov. Phys. Solid State **11**, 1403 (1969). [Tverd. Tela 11(6), 1730–1732 (1969)].
[19]R. Büscher and G. Lehmann, "Correlation of zero-field splittings and site distortions. IX. Fe^{3+} and Cr^{3+} in β-Ga_2O_3," Z. Naturforsch. **42**, 67 (1987).
[20]M. E. Ingebrigtsen, J. B. Varley, A. Y. Kuznetsov, B. G. Svensson, G. Alfieri, A. Mihaila, U. Badstübner, and L. Vines, "Iron and intrinsic deep level states in Ga_2O_3," Appl. Phys. Lett. **112**, 042104 (2018).
[21]J. L. Lyons, "A survey of acceptor dopants for β-Ga_2O_3," Semicond. Sci. Technol. **33**, 05LT02 (2018).
[22]C. A. Lenyk, T. D. Gustafson, S. A. Basun, L. E. Halliburton, and N. C. Giles, "Experimental determination of the (0/−) level for Mg acceptors in β-Ga_2O_3 crystals," Appl. Phys. Lett. **116**, 142101 (2020).
[23]S. Bhandari and M. E. Zvanut, "Optical transitions for impurities in Ga_2O_3 as determined by photo-induced electron paramagnetic resonance spectroscopy," J. Appl. Phys. **127**, 065704 (2020).
[24]B. E. Kananen, L. E. Halliburton, K. T. Stevens, G. K. Foundos, and N. C. Giles, "Gallium vacancies in β-Ga_2O_3 crystals," Appl. Phys. Lett. **110**, 202104 (2017).
[25]N. T. Son, Q. D. Ho, K. Goto, H. Abe, T. Ohshima, B. Monemar, Y. Kumagai, K. Frauenheim, and P. Deak, "Electron paramagnetic resonance and theoretical study of gallium vacancy in β-Ga_2O_3," Appl. Phys. Lett. **117**, 032101 (2020).
[26]D. Skachkov, W. R. L. Lambrecht, H. J. von Bardeleben, U. Gerstmann, Q. D. Ho, and P. Deák, "Computational identification of Ga-vacancy related electron paramagnetic resonance centers in β-Ga_2O_3," J. Appl. Phys. **125**, 185701 (2019).
[27]T. D. Gustafson, C. A. Lenyk, L. E. Halliburton, and N. C. Giles, "Deep donor behavior of iron in β-Ga_2O_3 crystals: Establishing the $Fe^{4+/3+}$ level," J. Appl. Phys. **128**, 145704 (2020).
[28]E. Korhonen, F. Tuomisto, D. Gogova, G. Wagner, M. Baldini, Z. Galazka, R. Schewski, and M. Albrecht, "Electrical compensation by Ga vacancies in Ga_2O_3 thin films," Appl. Phys. Lett. **106**, 242103 (2015).